Experimental and numerical analysis of a thermoplastic lamina for composite material

Available online at www.sciencedirect.com

ScienceDirect

Procedia Structural Integrity 24 (2019) 11–27

Structural Integrity Procedia

www.elsevier.com/locate/procedia

AIAS 2019 International Conference on Stress Analysis

Experimental and numerical analysis of a thermoplastic lamina for composite material

Dario Fiumarella[a], Simonetta Boria[b], Giovanni Belingardi[a], Alessandro Scattina[a]*

[a]*Department of Mechanical and Aerospace Engineering, Politecnico di Torino, 24 Duca degli Abruzzi, 10121, Torino, Italy.*
[b]*School of Science and Technology, University of Camerino, 9 Madonna delle Carceri, 62032, Camerino, Italy.*

Abstract

Thermoplastic composites nowadays belong to an interesting class of materials for different type of industries. Those materials present a considerable number of advantages compared to the thermosetting composites. Their low density, low production cost, recyclability, are some of the positive aspects encouraging their usage. The numerical simulation is still an open research field due to the peculiar behaviour of the thermoplastic composites. According to that, this works starts a detailed numerical study in which the main deformation mechanisms are simulated using different modelling approaches. In this overview, the object of this study is a fully polypropylene composites made up of woven polypropylene laminas. These laminas are stacked and hot pressed. Previous research showed a ductile and plastic crush behaviour of this material, in which the main failure mode is governed by the delamination. Firstly, an experimental campaign is carried out, in order to define the constitutive properties of the single lamina. Woven laminas are orthotropic composites responding differently according to the direction of the load. Yarn test was executed to capture the tensile modulus and the strength, whereas the Bias-Extension test was carried out to examine the in-plane shear properties. The definition of those properties required several considerations and a detailed analysis because the load applied in the test is directed neither along the weft nor along the wrap direction. For this reason, geometrical approximations and hypothesis about the boundary condition are necessary to evaluate the shear stress and the shear angle parameters. Hence, three different FE models were developed in LS-DYNA and results were validated against the experimental tests. Two geometry discretization method and three material models were implemented. The first numerical model was developed for fabric materials and it represents a macro-mechanics approach with low computationally cost. The second model instead accounts for the fabric architecture, allowing to evaluate the weave geometry and the reorientation effect of the yarns during the deformation. The third model represents the discrete architecture of the fabric, modelling the specimen at the tape level. The numerical results showed a good approximation of the experimental evidence, especially considering the second numerical model. This material model confirmed the geometrical assumptions used to define the mechanical properties. This work gives a first important step for the simulation of components made of thermoplastic composites and with more complex geometry using a mesoscopic approach.

Peer-review under responsibility of the AIAS2019 organizers
10.1016/j.prostr.2020.02.002

Keywords: composite lamina; thermoplastic composite; thermoplastic woven fabric; bias-extension test; numerical simulation; experimental tests.

1. Introduction

Thermoplastic composite materials are nowadays a challenging topic to face. The advantages of this class of material are confirmed from many researches (Muzzy et al. 1984, Campbell 2004, El-Sonbati 2012). Firstly, thermoplastic composite material can be easily recycled due to the possibility to reheat and reshape them. This is a fundamental characteristic concerning, in particular, the automotive field, in which restrictive regulations and recycle threshold are imposed (Directive 2000/53/EC). Furthermore, the lightweight of this class of material together with their structural behavior, makes them a suitable alternative to the actual thermosetting composite materials. Boria et al. (2019) experimentally compared the failure behavior of a composite material made up of stacked and hot-pressed thermoplastic laminas and thermosetting specimens. The thermosetting samples shown a different failure mechanism respect to the thermoplastic ones, in which the failure mode is mainly dominated by delamination.
The numerical modelling is a key step in the design phase in particular for the automotive components. Moreover, for the thermoplastic composites, the numerical modelling is still an open point to face, due to their peculiar mechanical and failure properties (Sun et al. 2018). Generally speaking, the thermoplastic composites are made up of a set of thermoplastic laminas, that can be considered the constitutive elements of the final composite. In this context, numerical models of the constitutive element of the thermoplastic composite are necessary in order to build reliable and low time-consuming models that can capture the failure behavior of the whole composite. In this work, the thermoplastic woven lamina that composes the final composite material is experimentally and numerically investigated. The numerical models of the composite lamina are then validated against the experimental tests.
Due to their peculiar constitutive architecture, woven fabric presents anisotropic and non-linear characteristics. The mechanical behavior of a woven fabric is complex due to the intricate yarns interaction mode that influences its global behavior. The multi-scale nature of the fabric inquires simulation techniques different from those of numerical models that represents continuous materials. Komeili et al. (2011) defined the hierarchical levels through which a woven fabric can be scaled. At the macroscopic level, the fabric is considered as a continuous medium. At the mesoscopic level the fabric woven architecture is captured, and the yarns are considered homogeneous. At the microscopic level, each yarn is further discretized as a set of micro-fibers. According to the level at which the fabric is discretized, different finite element modelling approaches and homogenization techniques can be implemented. Boisse et al. (2007) proposed a comparison between continuous and discrete modelling. Continuous models consider the whole fabric as an anisotropic material, with orthogonal or non-orthogonal material axes. The challenge of this macro-approach is to account for the yarn rotation during large deformations of the fabric. X.Q. Peng et al. (2005) developed a continuum non-orthogonal model for the characterization of the woven composite fabric. Stress and strain are transformed from the global orthogonal coordinate to the local non-orthogonal coordinate system. This transformation allows to trace the fiber reorientation during the deformation. The discrete method refers to the structural mechanics of the fabric. The fabric is considered as an assembly of their constitutive yarns. In this case, the directions of the yarns are naturally followed during the reorientation phases, since the geometry is modelled at the yarn scale. Boubaker et al. (2006) implemented a discrete approach by modelling the fabric unit cell as a truss of elastic beams connected by hinges with rotational stiffness. The fabric represents a mesoscopic view of the whole woven structure. Jauffres et al. (2009) built a discrete model of the unit cell using 1-D element as the edge of the cell and 2-D element as the central portion of the cell. The 1-D element accounts for the tensile contribution and follows the yarn rotation during the reorientation phase. The 2-D element supports only the shear resistance. However, the computational cost needed to simulate using the discrete technique is relevant, and this approach is restricted to simple geometry models.
This work proposes three different modelling approaches for the simulation of a thermoplastic woven lamina subjected to the bias-extension test using the FE code LS-DYNA. A low computational cost and a good agreement with the experimental results are the constraints for the model's set-up, looking forward to the implementation of those models to components with more complex geometry.
The paper is divided as follow. Firstly, the composite lamina is experimentally characterized. A discussion on the experimental tests used to characterize the lamina is proposed, focusing the discussion on the determination of the in-plane shear properties of the fabric. After that, three modelling techniques based on different model's discretization

are proposed. Finally, the numerical results are compared and validated against the experimental tests.

Nomenclature

μ	Discount Factor
E	Young Modulus
F_{sh}	Normalized Shear Force
G	Shear Modulus
PP	Polypropylene
RVC	Representative Volume Cell
$\Delta\vartheta$	Tolerance Angle for Locking
σ_{max}	Maximum tensile stress
υ	Poisson Ratio
γ	Shear Angle

* Alessandro Scattina. Tel.: +39-011-090-6900 ; fax: +39-011-090-6999 .
E-mail address: alessandro.scattina@polito.it

2. Material and Methods

2.1. Material

A balanced woven fabric made of a fully thermoplastic material was considered for the experimental test. The lamina is made up of all-PP tapes with an A:B:A structure. Those tapes are made of a core and two skins. The core is a PP homopolymer, whereas the skins are made of PP copolymer. Homopolymer and copolymer have different melting temperatures. Generally speaking, polymers presents a high degree of anisotropy at the molecular level. The mechanical properties of the polymers can be tuned and enhanced by orienting the polymer chain. Accordingly, the core is highly oriented, providing good strength performance. The skins have lower melting temperature than the core and they form the matrix of the composite material. The final tapes are then obtained using a co-extrusion process, after which the tapes are woven into fabrics (Figure 1). This fabric is hot-compacted to obtain the final composite sheets. The final composite obtained in this way is fully recyclable because both the matrix and the reinforcements are made of polypropylene. The production process of this all-PP composite material is patented, and it is known with the commercial name of PURE©. The geometrical properties of the PURE© tapes and lamina are summarized in table 1.

Figure 1: Surface detail of the final PURE© composite sheet. The fabric architecture can be noted.

Table 1: Pure lamina and tape properties.

Lamina Thickness (mm)	Lamina Density (kg/mm^3)	Tape Width (mm)	Tape Cross-Section (mm^2)
0,28	$7{,}2 \cdot 10^{-7}$	2,25	0,15

2.2. Experimental tests on lamina

The mechanical properties of the PURE© sheets and of the PURE© composite were largely investigated by the authors (Boria et al. 2015, 2018). The mechanical standard tests performed on this thermoplastic composite showed a high stiffness and strength together with a failure mode dominated by delamination. The material demonstrated a strain-rate sensitivity, since an increase of the elastic modulus occurred with the increasing of the test velocity. Quasi-static and dynamic crushing tests carried out on circular tubes made of PURE© showed a ductile response together with a high degree of energy absorption.

In this work, experimental tests on the single lamina were executed because they are fundamental to define the mechanical properties at the fabric level. Three experimental tests were carried out with an electro-mechanical testing machine (Zwick Z100): fabric tensile test, fabric bias-extension test and tensile test on single tapes. The clamping devices were designed by the authors for these specific tests in order to have a single couple of devices for the three type of tests.

The fabric tensile test was executed according to the Strip Method ASTM5035 standard. The specimens were prepared with hand cutting operation. The width of the specimens was 50 mm, and each side of the specimen was ravelled. An adhesive neoprene layer was inserted between the two surfaces of the clamping device in contact with the specimen in order to increase the friction and to avoid the sliding of the specimen.

The bias-extension test was executed for the in-plane shear characterization of the composite lamina. The bias extension test is an efficient and effective alternative to the picture-frame test, in which a specific trellis-gripper is necessary (Lomov et al. 2008). In the bias-extension test, the specimens were pulled in extension and the warp and weft tapes are oriented at 45° respect to the load application direction. According to the crosshead motion and to the geometrical assumptions that are discussed in section 3, it is possible to evaluate the shear angle and the shear stress. The dimension of the specimens was 260×120 mm. The initial length of the specimen must be more than twice its width as suggested by Boisse et al. (2017). If this condition is respected, there is a pure shear region in the central part of the specimen. Reference lines were drawn on the surface of the specimens as showed in Figure 2. The reference lines help to avoid misalignment of the yarn directions during the test setup according to the experimental campaign carried out by Cao et al. (2008). Furthermore, those lines were used as reference to measure the variation of the shear angle during the test. The test speed was set to 20 mm/min.

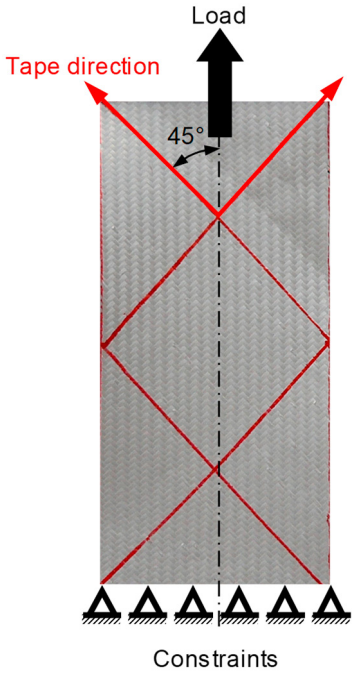

Figure 2: Sample for the bias-extension test.

The elastic modulus of the tape was evaluated performing a tensile test on a single-tape. Tapes were obtained from the whole fabric. The gauge length of the tested specimens was 70 mm. The clamping devices used for this type of test had a screw with hexagonal head inserted into a drilled pin. The tape was clamped between the screw head and the side face of the pin. The tightening torque applied to the screw must be higher enough to prevent the sliding of the specimen during the test. Nevertheless, a too high force could cause micro-lesions to the copolymer layer, leading to a premature damage of the tape.

2.3. FE Models

The constitutive properties of the lamina which were evaluated with the experimental tests were used to set-up three finite element models in order to simulate the bias-extension test. The simulations were executed using the FE software LS-DYNA in its explicit formulation. The aim of the FE simulations was to develop a numerical model able to capture the non-linear and the non-isotropic behaviour of the woven fabric subjected to the bias-extension test. The woven fabric presents usually two main modes of deformations: stretching of the fibres and in-plane shearing of the fabric (Jauffrès et al. 2010).

Two different modelling methodologies were developed as shown in Table 2. In the first type of models the specimen geometry was considered as a continuum. The fabric is then homogenized. The non-linear orthotropic behaviour was guaranteed by material cards based on equi-biaxial input. This approach can be accepted for models with simple geometry. In the second methodology, the specimen geometry was modelled using a discrete approach i.e. individual component of the fabric such as tapes were discretized. For all the models, the force is applied to the top edge nodes, while the bottom edge nodes were translationally and rotationally constrained.

Concerning the first modelling technique, two material models were considered. The first bias-extension test was simulated with the LS-DYNA material model MAT_FABRIC (MAT_34). This is a planar-orthotropic material model. It models the fabric at a macroscopic level, using the Hooke's law as the constitutive equations as stated by Hill et al. (2013). This material model allows the use of an elastic liner, able to reduce the tendency of the elements to be crushed. The ratio of the liner thickness to the total fabric thickness was set to 0.5. A flag to modify the membrane formulation for fabric materials was selected. For the simulation of the bias-extension test, a Green-Lagrange strain formulation was chosen. According to this formulation, the material axes are assumed to be orthogonal. (LS-DYNA user's manual, 2018).

The second material model used in this work was the MAT_MICROMECHANICS_DRY_FABRIC (MAT_235) developed by Tabei and Ivanov (Tabei et al. 2002). This material model defines the meso-mechanical behaviour of the fabric considering the interactions between the fibres. As discussed below, the model accounts for the reorientation of the yarns, allowing the simulation of a trellis mechanism before that the locking angle is reached. The constitutive element of this material model is the representative volume cell (RVC). It represents the periodic structure of the fabric at a meso-level. Each cell is divided into 4 sub-cells. In each sub-cell the yarn fundamental angles are defined, such as the braid angle and the undulation angle. The initial braid angle was set in this work to 45 degrees. The specimen was modelled using a fully integrated shell (ELFORM 16) with 10 mm of mesh size.

For the second modelling technique a discretization of the geometry was implemented, aimed to better capture the geometrical deformation of the specimen. The specimen was modelled at the tape level, and the tapes were considered as a homogeneous media. The interaction of each tapes at the fabric level influences the macro-mechanics properties of the whole specimen at the global-level. Accordingly, the isotropic material model plastic kinematic (MAT_003) was used to simulate the specimen. It is a cost-effective material card, and the basic parameters evaluated with the experimental tests can be used as input in the material model. Each yarn was meshed with 2 mm shell element. The element formulation chosen for this model was the Belytschko-Tsai (ELFORM 2).

Table 2: Characteristics of the FE models.

#	Geometry	Geometry modelling	Homogenization	Material model
1	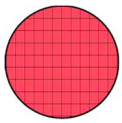	Continuum	Macro-Level. No yarn interaction	MAT 34
2	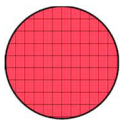	Continuum	Meso-Level. Yarn interaction accounted	MAT 235
3	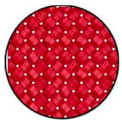	Discrete	Isotropic material	MAT 03

3. Results and Discussion

3.1. Experimental test

3.1.1 Tensile tests

Tensile test on three tapes were carried out, in order to evaluate the Young modulus of the material. The loading velocity was chosen aiming to avoid the sliding of the specimen. Accordingly, the testing speed was set to 2 mm/min The Figure 3 shows the load-displacement (A) and the stress-strain (B) curves. It is noticeable that the trend of the three curves S1 S2 and S3 is almost repeatable. The global behaviour of the material is hyperelastic, and a change in the slope is evident especially in the initial load path, until around 2 mm of stroke.

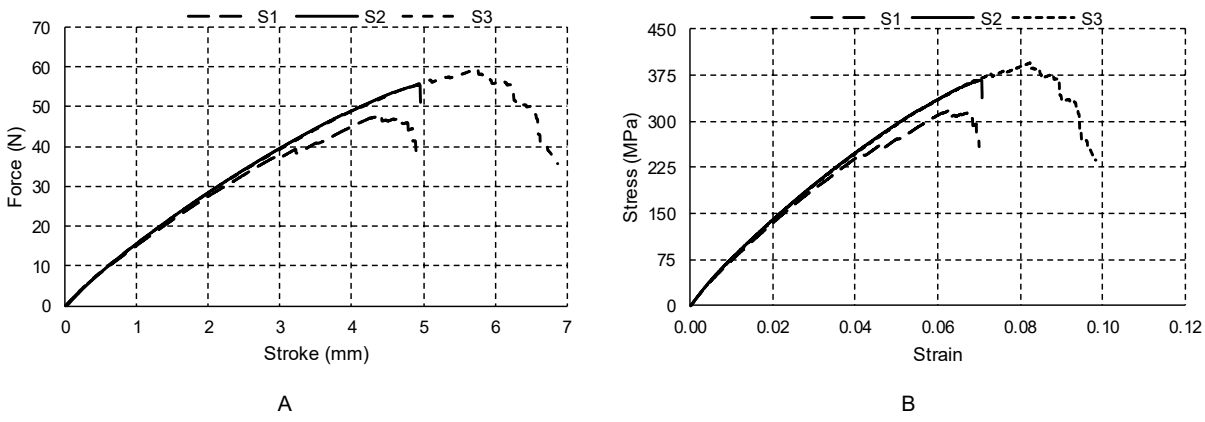

Figure 3: Experimental results of the tensile tests on the single tape: force-stroke (A) and stress-strain (B) curves.

The failure mode of the specimen was mainly dominated by delamination of the external skin (Figure 4B). The copolymer fibres firstly start to fail. Consequently, the area supporting the load decreases, and the stress increases.

After this phase, the skin stops contributing to the load bearing capability, and the core fails too (Figure 4C). The breaking force of the specimen S1 resulted much lower than the other two. From the S1 curve is also noticeable a scattered trend around 3 mm stroke. This trend is probably due to a lesion of the external skins since the tape was tightened with an excessive screwing torque. Therefore, the edge of the screw's head damaged the external skin of the tape, and a premature failure occurred.

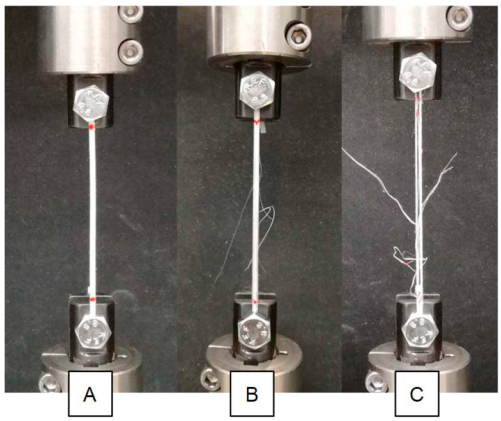

Figure 4: Sequence of the tensile test on the single tape. A) Undeformed tape. B) Copolymer starts to delaminate C) Homopolymer failure.

Tensile test on the woven fabric was also performed. With this tensile test the Poisson ratio of the fabric was estimated. The ASTM5035 was taken as guideline for the setting of the test parameters, even if a higher gauge length was considered respect to the value suggested by the standard. Excessive sliding between the grips and the fabric was evidenced in the specimens in which the gauge length suggested by the standard was used, making shrinkage impossible to be evaluated.

Table 3: Properties of the lamina and the tape obtained with the experimental tests.

Test type	Calculated Parameter	Value
Fabric Tensile Test	υ	0.42
Single Tape Test	E	5400 MPa
Single Tape Test	σ_{max}	380 MPa

3.1.2 Bias-Extension Test

The mechanical properties of the lamina subjected to shear deformation were captured with the bias extension test. The in-plane shear deformation of the woven fabric is the principal deformation mode obtained in this test. When a fabric is loaded in direction different from the weft and warp, a shearing deformation is induced. Accordingly, three main stages can be distinguished during the in-plane shear deformation, as shown in Figure 5.

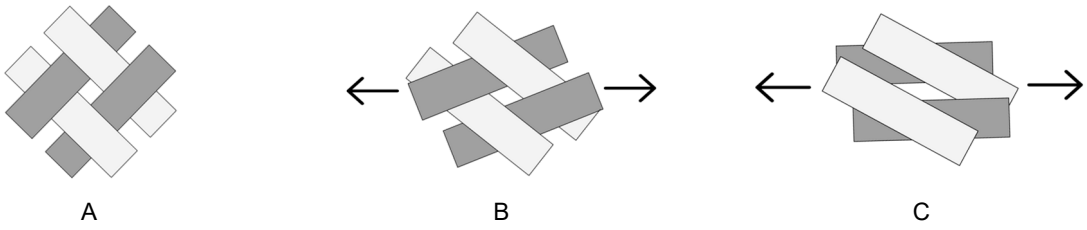

Figure 5: Deformation stages during the bias-extension test.

Figure 5A shows the initial state of the reference unit cell of a balanced woven fabric. The tapes are perpendicular to each other, and no deformation-state is induced. When a load is applied with an off-set angle to the direction of the interlacing orthogonal yarns (Figure 5B), the effect is to cause the angle between the two sets of yarn to decrease. The load is mainly due to the friction interaction between two crossed yarns. After this stage, the yarns start to compact as shown in Figure 5C. The compaction of the yarns causes a sharp increase of the force. At this point of the test, the yarn's angle is called locking angle (Morris et al, 2013). Increasing the load, the tapes are almost parallel, and a tensile load is induced. The force further increases, and the whole fabric starts to wrinkle.
This deformation mechanism can be well captured by two experimental tests: the picture-frame test and the bias-extension test. The first test involves the usage a trellis-frame to generate a shear-deformation state in a squared specimen. The second test is performed as a tensile test in which the yarns are oriented at 45° than the direction of the load. According to Morris et al. (2013), if the length of the specimen is at least the double of the width, 3 different deformation zones are induced in the specimen (Figure 6).

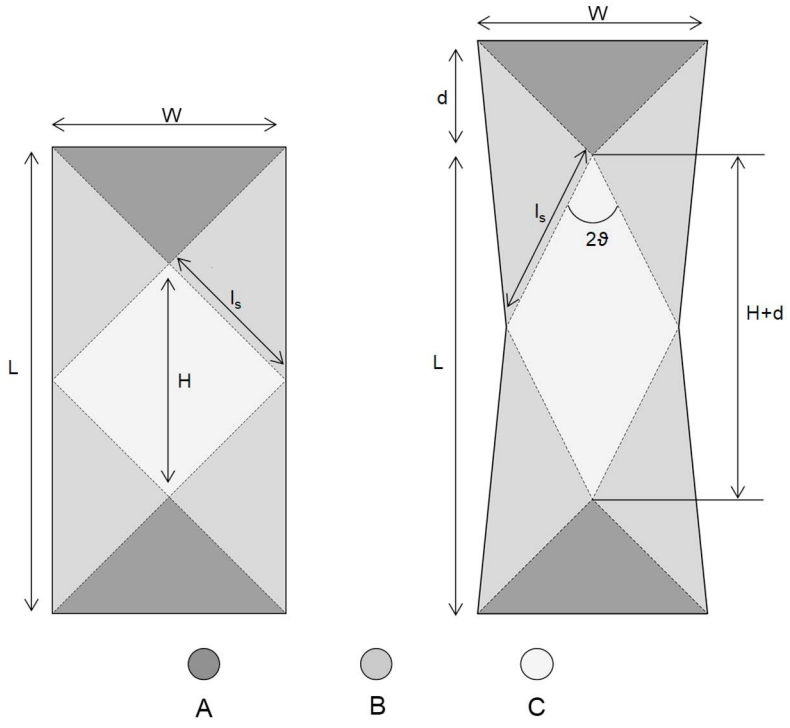

Figure 6: Deformation zones of the specimen during the bias-extension test.

The top edge of the zone A is fixed to the clamping devices and if the yarns are inextensible, no shear deformation is induced in the region A during the test. The zone C in subjected to pure shear and it behaves as a trellis mechanism. The shear-deformation in the zone B is assumed to be half than the one in the region C (Taha at al. 2012).
The Figure 7 shows a sequence of the specimen subjected to the bias-extension test. The zones A, B and C are clearly noticeable.

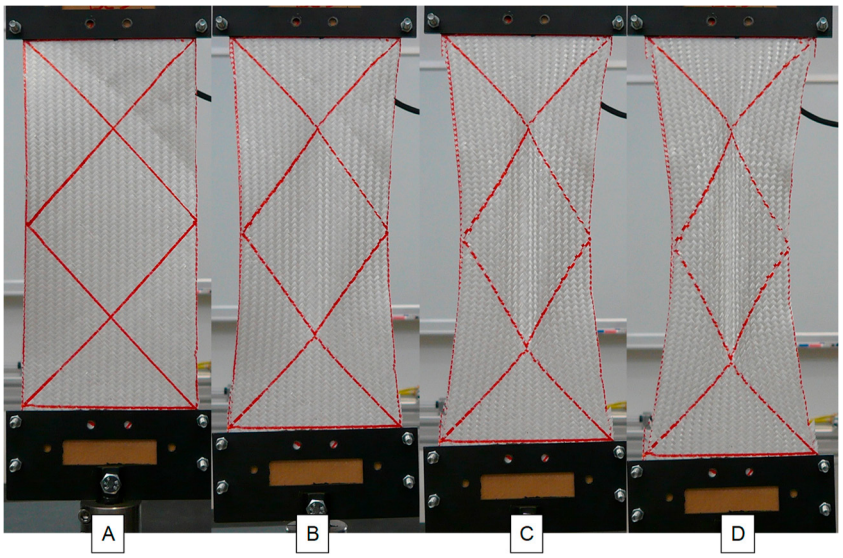

Figure 7: Sequence of stages during the bias extension test.

Figure 7A shows the undeformed specimen. As soon as the load was applied, the yarn re-orientation started in the central zone (Figure 7B). After the first stage, the compaction of the tapes caused the shear-locking (Figure 7C). At this point, an out-of-plane deformation can be noticed in the central zone. In the last stage (Figure 7D), the wrinkling of the tape occurred, and the load sharply increased.

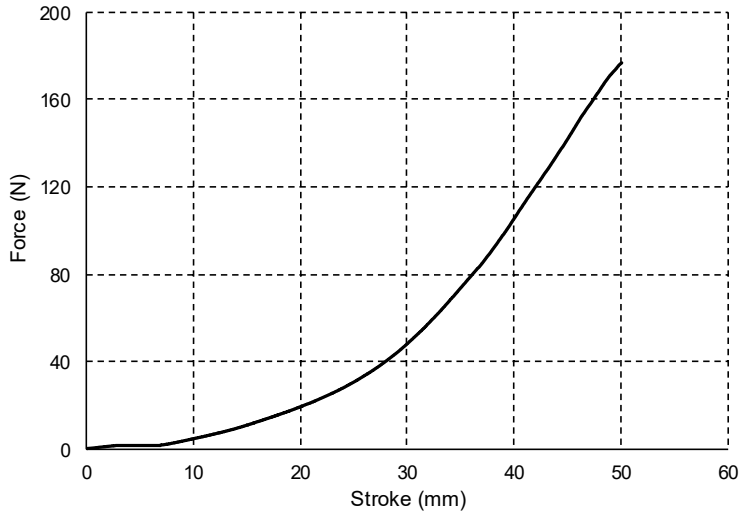

Figure 8: Force-Stroke trend of the bias-extension test performed on the PURE© fabric

The load-stroke trend of the bias-extension test is plotted in Figure 8. However, the global parameters obtained from this test are insufficient to evaluate the shear properties. Accordingly, geometrical considerations must be introduced to evaluate the shear behaviour of the specimen (Launay et al. 2008).
In the undeformed configuration, it is possible to write the length of the side edge of the zone C (Figure 6) as in equation (1):

$$l_s = H \cdot \frac{\sqrt{2}}{2} \tag{1}$$

where

$$H = L - W \tag{2}$$

If the length is exactly the double of the width, the equation (2) becomes

$$H = W \tag{3}$$

When a load is applied, the length of the specimen is extended of *d*. The A zones (Figure 6) are undeformed, and therefore only the *H* distance changes:

$$H + d = 2l_s \cdot \cos(\vartheta) \tag{4}$$

Consequently, it is possible to evaluate the ϑ angle (Figure 6) as follows:

$$\vartheta = \cos^{-1} \frac{L - W + d}{(L - W) \cdot \sqrt{2}} \tag{5}$$

The shear angle γ in the zone subjected to pure shear (zone C) can be evaluated with the equation (6):

$$\gamma = \frac{\pi}{2} - 2\vartheta \tag{6}$$

Considering the parameter *d* as the stroke obtained during the bias-extension test, it is possible to plot the shear angle as a function of the applied load, as shown in Figure 9.

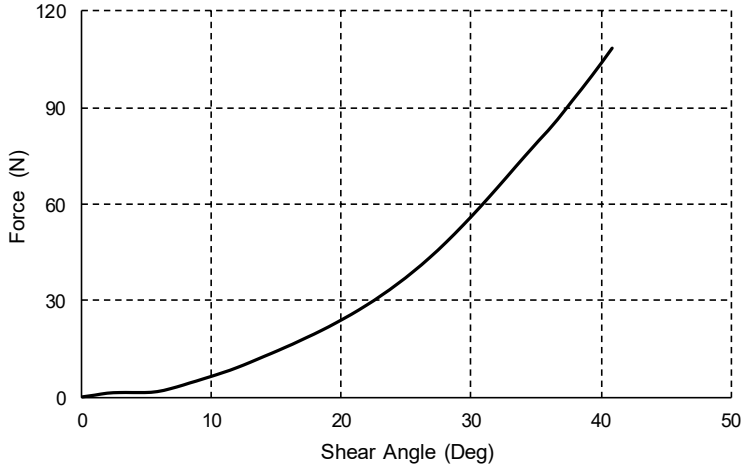

Figure 9: Trend of the force as a function of the shear angle obtained during the bias extension test.

Cao et al. (2008) compared the theoretical shear angle, with the shear angle measured with an image-correlation software. The results showed that the difference between the true shear angle and the theoretical one became larger after 30°. Accordingly, for the next evaluations the data after this angle will be discarded. From the Figure 9 a change of slope can be noticed at around 8 mm of stroke. This change of the trend is due to the yarn lock effects.
After the conversion of the experimental force-stroke curve to a force-shear angle curve, a recursive process can be used to evaluate the normalized shear force F_{sh}. The F_{sh} is the load independent from the dimensions of the considered sample, and it can be evaluated starting from the pull force with the following equation (Figure 5):

$$F_{sh}(\gamma) = \frac{1}{(2L-3W)\cos\gamma}\left(\left(\frac{L}{W}-1\right)\cdot F\cdot\left(cos\frac{\gamma}{2}-sin\frac{\gamma}{2}\right)-W\cdot F_{sh}\left(\frac{\gamma}{2}\right)cos\frac{\gamma}{2}\right) \text{ (Cao et al. 2008)} \quad (7)$$

The function $F_{sh}(\gamma)$ depends on the function itself evaluated in $\left(\frac{\gamma}{2}\right)$. Hence, it is necessary to impose the initial condition of the recursive algorithm; a very small shear angle was considered as boundary condition:

$$F_{sh}(\gamma \to 0) = 0 \quad (8)$$

Figure 10 shows the trend of the normalized shear force as a function of the shear angle. The locking angle is around 5°, where there is an evident change of the slope of the curve. With the normalized shear force, it is possible to calculate the shear stress as function of the shear angle, dividing the F_{sh} by the thickness of the fabric (Samir et al. 2014).
From the chart of shear stress as a function of the shear angle (in radiant, Figure 11), three change of slope are well evidenced. The region R1 is the reorientation region. The region R2 is the after-locking zone, in which the compaction of the tape occurs, and the force sharply increases. In the last part of the curve (R3), the yarns started to support the tension loads and the slope of the curve further increases. Each slope of the curve corresponds to a different shear modulus. The three portions of the curve were linearly interpolated, and the G_{12} value was obtained by calculating the slope of the interpolation line (Table 4).

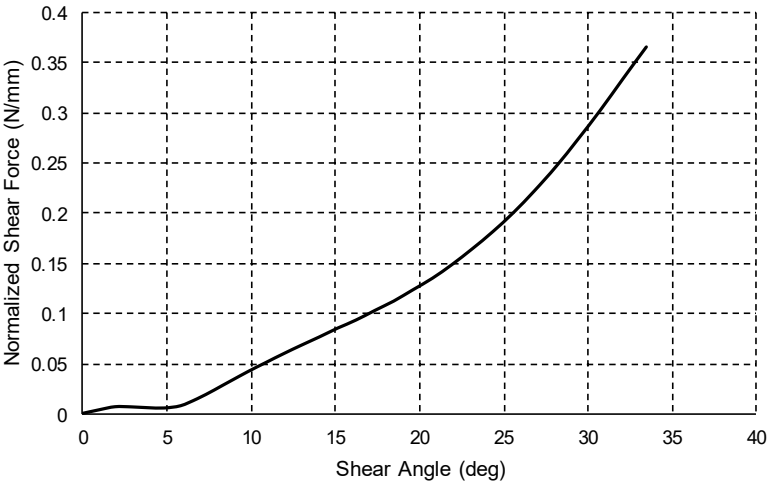

Figure 10: Trend of the normalized shear force as a function of the shear angle.

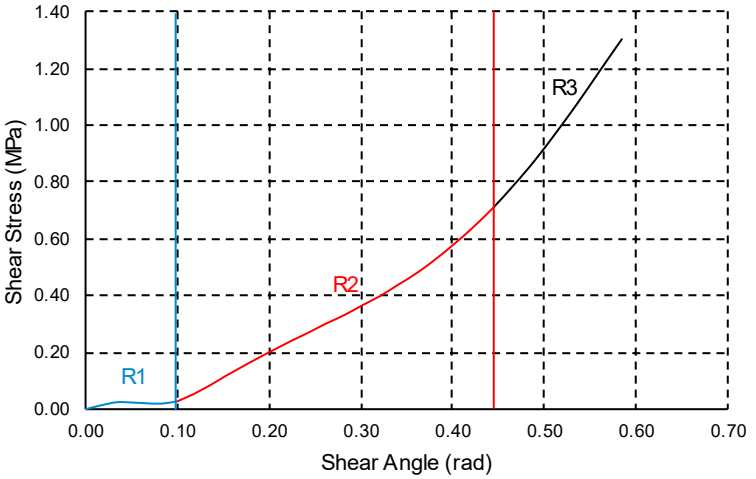

Figure 11: Trend of the shear stress as a function of the shear angle.

Table 4: Shear modulus of the PURE© lamina

G_{R1} (MPa)	G_{R2} (MPa)	G_{R3} (MPa)
0,2	1,7	4,1

3.2. Numerical Simulations

The mechanical properties evaluated with the experimental tests were used as starting parameters to set-up the input data for the material card in the numerical simulation. The material model MAT_FABRIC was suited for this task since it can capture the behaviour of the woven fabric considering it as an orthotropic material with the two main directions perpendicular to each other. The material axes were rotated of 45° respect to the load direction, as in the experimental test.
This material model demonstrated a high sensitiveness to the characteristics of the elastic liner. The absence of this caused an excessive wrinkle with a consequent compressive failure of the element in the zone C. The thickness of the liner was tuned by trial and error procedure in order to better capture the experimental evidence. Higher thickness caused an excessive stiffness of the specimen. Smaller thickness led the elements of the C region to a compressive failure.
The homogenization carried out by this material model makes it computationally desirable (Hill et al, 2013), and test with different mesh size could be executed without affecting the computation time in a marked way. Therefore, two simulations with different mesh size were executed. In the Figure 12 the comparison between the experimental curve and the numerical one is shown. The curve obtained with a 10 mm mesh size is labelled MAT_34_B, whereas the curve obtained with a 5 mm mesh size is labelled MAT_34_F. The difference between the two numerical curves confirmed a strong mesh sensitiveness of the model. The model with 5 mm mesh size seems to better capture the maximum load at 50 mm of displacement, even if the shape of the curve presents an opposite concavity. As a matter of fact, this material model ignores the mesoscopic interactions between the yarns, neglecting the reorientation effects and their influence on the global response of the fabric.

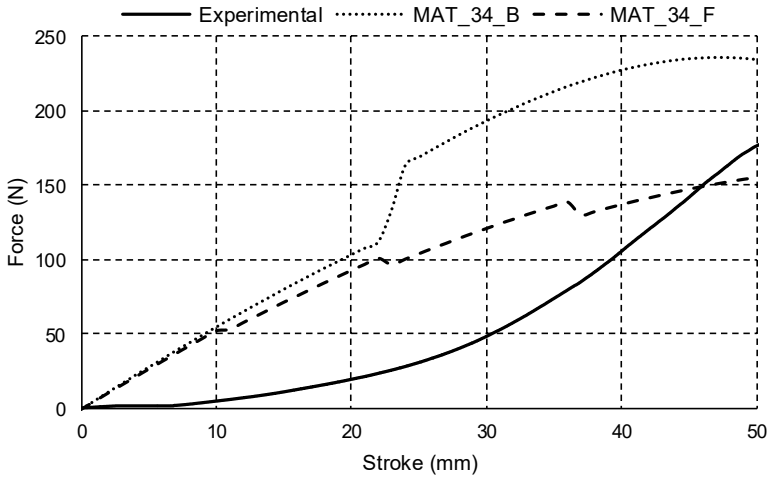

Figure 12: Comparison between the numerical results obtained with the MAT_FABRIC and the experimental one.

The material model micromechanics dry fabric (MAT_235) is a micromechanics-based model that accounts for the reorientation effect of the yarns and their locking (Tabei et al. 2002). This material model implements the detailed architecture of the fabric simulating it as a trellis mechanism. The Young modulus, Shear modulus, Poisson ratio and the locking angle were tuned according to the experimental tests. The elastic modulus of the weft (E_1) and warp (E_2) directions, were considered equal. The other parameters of the material card were calibrated by trial and error approach.
The discount factor μ demonstrated high influence on the simulation results. The discount factor scales down the shear resistance before the locking angle is reached. It simulates the low shear resistance at the very beginning of the yarn

rotation. Higher μ value increases the slope of the R1 region. The figure 13 compares two different value of discount factor. The μ_1 is one order of magnitude lower than the μ_2. It is evident that the force in the simulation with the μ_2 value starts to markedly rise around 10 mm before than the curve with the μ_1 value. A very small discount factor was set for the simulation to better capture the slope of the first region of the experimental curve.
The tolerance angle for locking $\Delta\vartheta$ had a strong influence on the simulation results too. Its effect is to smooth the transition between the unlocked and the locked region. The adjust of this factor further improve the fit of the numerical results with the experimental data.
In the Figure 14 the comparison between the experimental curve and the numerical one is shown. It is possible to notice a good approximation of the FE curve, especially in the locking region. When the locking angle is reached at 5° (at about 8 mm of stroke), both curves start to rise.

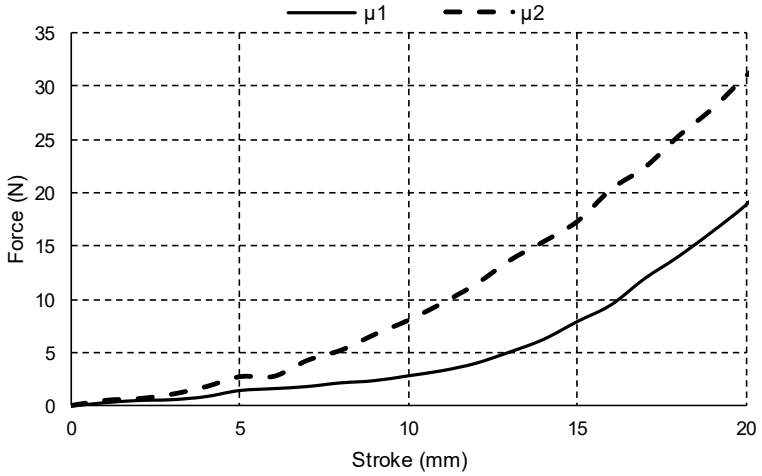

Figure 13: Detail of the first region of the numerical curve. The effect of the discount factor is evidenced.

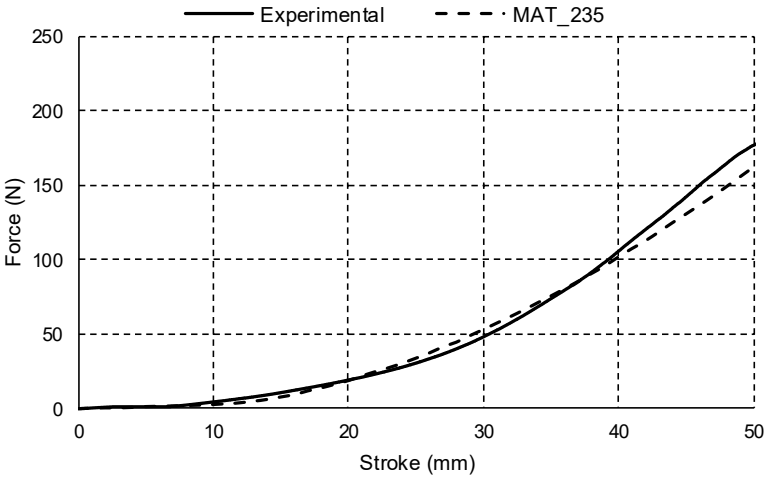

Figure 14: Comparison between the numerical results obtained with the MAT_MICROMECHANICS_DRY_FABRIC and the experimental one.

Geometrical considerations about the meso-scale deformation of the specimens can be done by considering a model that discretizes the architecture of the sample at the tape level.

The Figure 15 shows a comparison between the experimental specimen and the simulation performed with the discretized model. Each tape was meshed with quad element with an average size of 2 mm, and the automatic single surface card was selected in order to impose contacts between the yarns. The results comparison confirmed the good accordance of the geometrical deformation during the test between experimental and FE model. The out-of-plane deformation of the C region was well captured by the FE model, as well as the yarn behaviour at the edge of the sample (Figure 15). Furthermore, the Figure 16 confirmed the considerations about the three deformation regions during the bias-extension test. The region A remains undeformed during the test, while displacements slowly growths moving towards the central zone.
The material model plastic kinematic (MAT_03) was suited for this simulation. As matter of the fact, a simple isotropic model was enough to simulate the behaviour of the sample during the bias-extension test, since the orthotropy and the fabric architecture was guaranteed by the geometry discretization. The input parameters were the yarn elastic modulus, the density and the Poisson modulus. The test results are shown in the Figure 17.

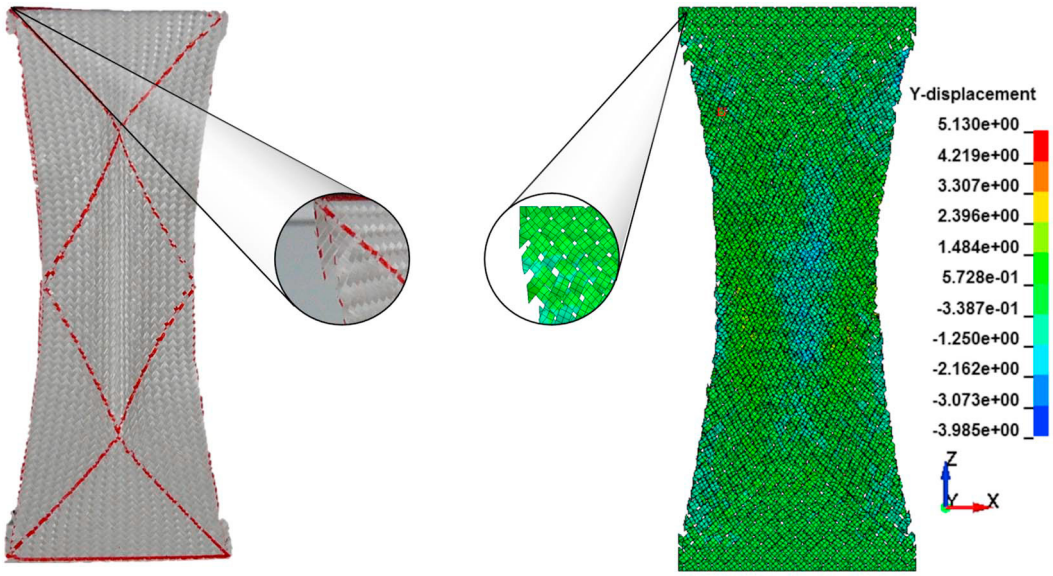

Figure 15: Comparison of the geometrical deformation between experimental and numerical results. In detail the two deformed edges.

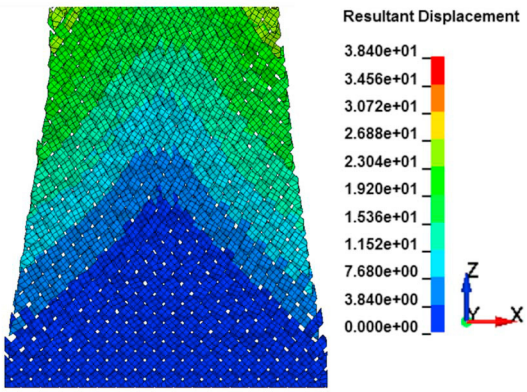

Figure 16: Detail of the A region. The resultant displacements are shown.

Although the maximum load at 50 mm of stroke is well captured by the numerical curve, the differences of the global trend of the curve are not negligible. The reorientation region of the numerical model lasts till 30 mm of stroke. Subsequently, the locking angle is reached, and the load sharply increases. This marked difference is due to the low shear-stiffness of the model. During the reorientation phase, the tapes are unconstrained and can rotate freely. This condition led the force to remain approximately at zero, until the yarns start to support the tensile load. After the *L* point (Figure 17) the force rapidly rises and consistent out of plane deformation in the C region occurs.
The static friction coefficient *FS* in the control card of the contact demonstrated to influence the force trend of the numerical model and can be tuned by trial and error accordingly. Increasing the *FS* coefficient, the point at which the curve starts to raise moves at lower displacements.

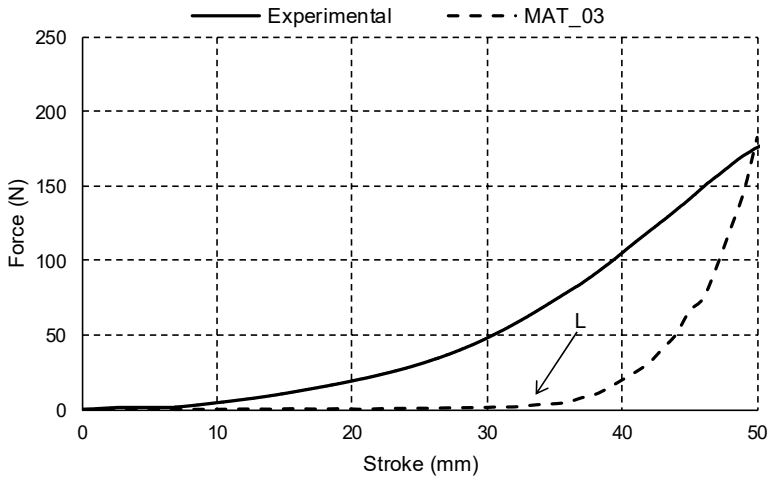

Figure 17: Comparison between the discrete model numerical and experimental curve. L indicates the point of the stroke at which the locking of the numerical model occurs.

4. Conclusion

A comparison between three finite element models for the simulation of a lamina for thermoplastic composite was presented. The work was based on data obtained from experimental tests. Due to the mechanical properties, lightweight and recyclability, the application of thermoplastic composites in the automotive field is nowadays of great interest. The inquired material was an all-PP lamina of a composite material named PURE©, produced with a patented process. The data coming from the tensile test on a single tape, fabric tensile test and bias-extension test were the constitutive properties used as input for the numerical model of the lamina. Moreover, a recursive algorithm based on geometrical assumptions was implemented to extrapolate the shear properties of the fabric subjected to the bias-extension test. Yarn reorientation, compaction and yarn locking influenced the shear properties of the fabric. Accordingly, three different shear modules were evaluated with the experimental shear stress-shear angle curve.
The properties obtained with the bias-extension test were validated using the FE software LS-DYNA, modelling the specimen according to different discretization of the geometry and different material models. The material model micromechanics dry fabric (MAT_235) could match the experimental results more precisely than the other material models. The parameters accounting for the meso-architecture of the fabric and for the yarn reorientation effects were tuned by trial and error procedure. Nevertheless, the increased computational cost compared with the material model fabric (MAT_34) makes it suited for the simulation of components with simple geometry. The material model fabric (MAT_34) demonstrated lower agreement with the experimental results, even if its reduced number of input parameters and lower computational time makes it desirable for a large-scale usage. The numerical simulation based on the discretization of the geometry at the yarn level of the sample, was able to capture the out-of-plane deformations occurred during the bias-extension test. However, the global force-displacement trend had important discrepancy respect to the experimental one, due to the tricky tuning of the yarn-interaction parameters that influence the shear

behaviour of the specimen. Furthermore, the higher computational cost and the intricate discretization of the geometry makes this model the less effective of the three models examined in this work.
The results of this work can be used as starting point for the simulation of the whole PURE© thermoplastic composite. The model implementing the material model micromechanics dry fabric (MAT_235) was defined as the best solution to simulate the failure mode of a simple PURE© specimen.

References

Boisse, P., Hamila, N., Guzman-Maldonado, E., Madeo, A., Hivet, G., dell'Isola G., 2017. The bias-extension test for the analysis of in-plane shear properties of textile composite reinforcements and prepregs: a review. International Journal of Material Forming 10(4), pp.473-492.

Boisse, P., Hamila, N., Helenon, F., Hagege, B., Cao, J., 2008. Different approaches for woven composite reinforcement forming simulation. International Journal of Material Forming 1, 21-29.

Boria, S., Belingardi, G., Fiumarella, D., Scattina, A., 2019. Experimental crushing analysis of thermoplastic and hybrid composites. Composite Structures 226, 111241.

Boria, S., Scattina, A., 2018. Energy absorption capability of laminated plates made of fully thermoplastic composite. Journal of Mechanical Engineering Science 232, 1389-1401.

Boria, S., Scattina, A., Belingardi, G., 2015. Experimental evaluation of a fully recyclable thermoplastic composite. Composite Structures 140, 21-35.

Boubaker, B.B., Haussy, B., Ganghoffer, J.F., 2006. Discrete models of woven structures. Macroscopic approach. Composites: Part B 38, 498-505.

Campbell, F.C., 2004. Thermoplastic Composites: An Unfulfilled Promise. In: Manufacturing Processes for Advanced Composites. Elsevier Science, pp. 357.

Cao, J., Akkerman, R., Boisse, P., Chen, J., Cheng, H.S., de Graaf, E.F., Gorczyca, J.L., Harrison, P., Hivet, G., Launay, J. Lee, W., Liu, L., Lomov, S.V., Long, A., de Luycker, E., Morestin, F., Padvoiskis, J., Peng, X.Q., Sherwood, J., Stoilova, Tz., Tao, X.M., Verpoest, I., Willems, A., Wiggers, J., Yu, T.X., Zhu, B., 2008. Characterization of mechanical behavior of woven fabrics: experimental methods and benchmark results. Composites Part A: Applied Science and Manufacturing 39(6), pp.1037-1053.

Directive 2000/53/EC of the European Parliament and of the Council of 18 September 2000 on end-of life vehicles. Official Journal of the European Communities (21 October 2000)

El-Sonbati, A.Z., 2012. Thermoplastic – Composite Materials. InTech, Croatia.

Hill, J.L., Braun, R.D., 2013. Implementation of a Mesomechanical Material Model for IAD Fabrics within LS-DYNA. AIAA Aerodynamic Decelerator Systems (ADS) Conference. Daytona Beach, Florida.

Jauffrès, D., Sherwood, J.A., Morris, C.D., Chen, J., 2009. Discrete mesoscopic modelling for the simulation of woven-fabric reinforcement forming. International Journal of Material Forming 3, 1205-1216.

Komeili, M., Milani, A.S., 2011. Finite element modelling of woven fabric composites at meso-level under combined loading modes, in "Advances in modern woven fabrics technology". In: Savvas Vassiliadis (Ed.). IntechOpen.

Launay, J., Hivet, G., Duong, A.V., Boisse, P., 2008. Experimental analysis of the influence of tensions on in plane shear behaviour of woven composite reinforcements. Composite Science and Technology 68, pp. 506-515.

Lomov, S.V., Boisse, P., Deluycker, E., Morestin, F., Vanclooster, K., Vandepitte, D., Verpoest, I., Willems, A., 2008. Full-Field strain measurements in textile deformability studies. Composites: Part A 39, 1232-1244.

LSTC, LS-DYNA. Keyword User's Manual, 2018. R11, LSTC, Livermore, California.

Morris, C., Dangora, L., Sherwood, J., 2013. Using LS-DYNA to simulate the forming of woven-fabric reinforced composites, 19th international conference composite materials. Montreal, Canada.

Peng, X.Q., Cao, J., 2005. A continuum mechanics-based non-orthogonal constitutive model for woven composite fabrics. Composites Part A 36, 859-874.

Samir, D., Satha, H., 2014. Determination of the in-plane shear rigidity modulus of a carbon non-crimp fabric from bias-extension data test. Journal of composite materials 48, pp. 2729-2736.

Sun, X.C., Kawashita, L.F., Kaddour, A.S., Hiley, M.J., Hallett, S.R., 2018. Comparison of low velocity impact modelling techniques for thermoplastic and thermoset polymer composites. Composite Structures 203, 659-671.

Tabei, A., Ivanov, I., 2002. Computational micro-mechanical model of flexible woven fabric for finite element impact simulation. International journal for numerical methods in engineering 53, pp.1259-1276.

Taha, I., Abdin, Y., Ebeid, S., 2013. Comparison of Picture Frame and Bis-Extension test for the characterization of shear behaviour in natural fibre woven fabrics. Fibers and Polymers 14, pp. 338-344.